Diffusion tensor of water in model articular cartilage

Konstantin I. Momot*

Discipline of Physics, Queensland University of Technology,
GPO Box 2434, Brisbane, Qld 4001, Australia;
and
Institute of Health and Biomedical Innovation, Kelvin Grove,
Qld 4059, Australia

*Address for correspondence: Konstantin I. Momot
Discipline of Physics
Queensland University of Technology
GPO Box 2434
Brisbane, Qld 4001
Australia,
E-mail address: k.momot@qut.edu.au
Fax: +61 7 3138 1521

Running title: Water Diffusion Tensor in Cartilage

Revised version 9/08/2010 11:19 AM

Keywords: Diffusion tensor imaging; Monte Carlo simulations;
Nuclear Magnetic Resonance; cartilage; collagen; osteoarthritis

Abbreviations and symbols:

D, translational diffusion coefficient;

$||\mathbf{D}||$, diffusion tensor;

D_0, the translational diffusion coefficient in bulk water;

D_{ij}, element (i, j) of the simulated laboratory-frame diffusion tensor (e.g., D_{xy});

D_i, eigenvalues of the simulated laboratory-frame diffusion tensor;

DTI, diffusion-tensor imaging;

FA, fractional anisotropy of the diffusion tensor;

L_0 , size of the unit cell of the fibre lattice;

MC, Monte Carlo;

NMR, Nuclear Magnetic Resonance;

N_P, the number of tracer particles in a Monte Carlo random walk;

N_T, the number of time steps in a Monte Carlo random walk;

RMS, root-mean square;

$R_{x,y}$, radius of the fibre as measured in the x or y direction;

$\mathbf{r}_{mn}$, position of the n-th tracer particle at the end of the m-th time step;

$\mathbf{v}_i$, eigenvectors of the simulated laboratory-frame diffusion tensor;

Δ, diffusion time;

ΔD_i, the standard deviation of the simulated diffusion tensor eigenvalues;

$\Delta\mathbf{r}_{mn}$, displacement of the n-th tracer particle during the m-th time step;

Δt, time step in the random-walk simulation;

ϕ, volume fraction of collagen.

Abstract

We used Monte Carlo simulations of Brownian dynamics of water to study anisotropic water diffusion in an idealised model of articular cartilage. The main aim was to use the simulations as a tool for translation of the fractional anisotropy of the water diffusion tensor in cartilage into quantitative characteristics of its collagen fibre network. The key finding was a linear empirical relationship between the collagen volume fraction and the fractional anisotropy of the diffusion tensor. Fractional anisotropy of the diffusion tensor is potentially a robust indicator of the microstructure of the tissue because, in the first approximation, it is invariant to the inclusion of proteoglycans or chemical exchange between free and collagen-bound water in the model. We discuss potential applications of Monte Carlo diffusion-tensor simulations for quantitative biophysical interpretation of MRI diffusion-tensor images of cartilage. Extension of the model to include collagen fibre disorder is also discussed.

INTRODUCTION

Articular cartilage (AC) is a connective tissue that covers the articulating surfaces of movable joints in mammals. It plays a crucial role in biomechanical mobility of humans by reducing static contact stress in the joint and serving as a wear-resistant protective material for bones (Freeman 1979). The major components of cartilage are Type II collagen (15–20% of tissue weight) (Eyre and Wu 2005), proteoglycans (PG, 3–10%), and water (65-80%) (Freeman 1979; Xia 2000). The collagen forms a network of cross-linked fibres, in which three zones of alignment are usually distinguished: (1) the superficial zone, located near the articular surface, in which collagen fibres are aligned parallel to the surface; (2) the radial zone, located near the bone, in which the fibres are aligned normal to the bone; and (3) the transitional zone, which lies between the superficial and the radial zones and in which the collagen fibres are relatively disordered compared to the other two zones. This architecture of collagen fibres is responsible for the ability of cartilage to process mechanical load – i.e., to distribute the applied load to a greater contact area (Nieminen et al. 2004; Pierce et al. 2009).

The zonal structure and the alignment of collagen fibres in AC can be non-destructively observed in magnetic resonance diffusion-tensor imaging (DTI) (Azuma et al. 2009; Deng et al. 2007; Filidoro et al. 2005; Meder et al. 2006). Spatially-resolved maps of the direction of the principal eigenvector of the diffusion tensor have been shown to be consistent with the collagen alignment measured by other techniques, most notably polarised-light microscopy (PLM) (de Visser et al. 2008a). DTI has also been used to observe changes in collagen fibre orientation under mechanical compression (de Visser et al. 2008b; Pierce et al. 2010). However, to date the interpretation of DTI results in AC has been limited to the determination of the direction of the predominant alignment of collagen fibres, with no attempts to quantify the degree of alignment or the volume fraction of collagen – parameters that are also important for quantitative understanding of load processing in AC. One of the reasons for this is the lack of models that could enable translation of the fractional anisotropy of the diffusion tensor into quantitative morphological characteristics of the collagen network.

Monte Carlo (MC) modelling can provide valuable insights into the quantitative relationship between the tissue morphology and the measured diffusion tensor (Avram et al. 2008; Landman et al. 2010; Regan and Kuchel 2002). In this work, we used MC simulations of water diffusion in model cartilage as a tool that enables quantitative characterisation of the collagen fibre network

beyond merely determining the preferred direction of collagen alignment. The model comprised a regular network of identically aligned collagen fibres with a specified collagen volume fraction. Water molecules were assumed to undergo bulk water-like diffusion in the aqueous domain between the fibres; the diffusion was unobstructed in the direction of fibre alignment (taken as the z direction) but obstructed in the directions perpendicular to the fibres (x, y directions). We demonstrate that the fractional anisotropy of the simulated water diffusion tensor in this idealised model is a linear function of the volume fraction of collagen. We compare the simulation results with available experimental data and empirical models of restricted diffusion in collagen and related systems. We discuss limitations of the perfect-alignment model as well as its possible extension to include fibre disorder. We also discuss the feasibility of using the fractional anisotropy of the DT for probing the degree of alignment of collagen in articular cartilage.

METHODS

Monte Carlo simulations. The following physical units were used throughout this work: distance, millimetres (mm); time, seconds (s); translational diffusion coefficient, $mm^2\ s^{-1}$.

The translational self-diffusion tensor of water was computed from Monte Carlo (MC) simulations of 3D random walks of tracer water molecules in a regular square network of collagen fibres. The displacements of the tracer molecules at the end of the simulation were used to compute the corresponding diffusion tensor.

All fibres were modelled as straight and identically aligned. The direction of the alignment was taken as the *z* direction. The centres of the fibres formed a periodic square grid in the *xy* plane, as shown in Fig. 1. The size of the unit cell of the grid was taken as $L_0 = 10^{-4}$ mm in all simulations. The cross-sectional shape of the fibres in the lattice was defined as a trigonometric function-based approximant to the circle, as described in the Appendix. This enabled the modelling of an infinite fibre network and therefore obviated the need for periodic boundary conditions. The simulated collagen volume fraction (ϕ) was controlled via the collagen fibre threshold parameter (T) discussed in the Appendix. Water diffusion tensors were simulated for 17 values of the collagen volume fraction that were spaced approximately equidistantly and lay in the range from 0 to 0.41. For each value of ϕ, ten MC simulations were performed as described below. The diffusion tensors obtained from the sets of ten simulations were used to evaluate the uncertainties of the computed DT eigenvalues and fractional anisotropies.

Each MC simulation of model AC consisted of tracing the stochastic trajectories of $N_P = 81910$ tracer molecules over $N_T = 30000$ time steps. The duration of the time step used, $\Delta t = 5 \times 10^{-9}$ s, was selected such as to ensure that the length of each random-walk step was much smaller than both L_0 and the cross-sectional radius of the fibre ($R_{x,y}$): $\Delta t << L_0^2/2D_0,\ R_{x,y}^2/2D_0$. This requirement was imposed in order to avoid the tracer molecules "skipping" the fibres, which would have resulted in an under-estimated fractional anisotropy of the diffusion tensor. At the beginning of each simulation, the tracer particles were given random initial positions $\mathbf{r}_{0n}$ that were uniformly distributed in the aqueous domain of the unit cell confined between $x = 0$, $x = L_0$ and $y = 0$, $y = L_0$, as illustrated in Fig. 1a. This ensured a uniform and representative sampling of the pore space. The initial *z* positions were zero for all tracer particles. The duration of the

simulation, $\Delta = N_T \times \Delta t = 1.5 \times 10^{-4}$ s, was chosen such as to ensure that the average magnitude of particle displacement significantly exceeded the period of the fibre lattice. This, in turn, ensured that the diffusion tensor sampled in the simulations corresponded to the asymptotically long diffusion time (see Discussion). A typical distribution of the tracer particles at $t = \Delta/20$ is illustrated in Fig. 1b.

In each time step of the simulation, each tracer molecule attempted a step of fixed length

$$\Delta r = \sqrt{6 D_0 \, \Delta t} \tag{1}$$

where $D_0 = 2.3 \times 10^{-3}$ mm^2 s^{-1} was the self-diffusion coefficient of water molecules in bulk water at 25 ^{o}C. The direction of the attempted displacement vector of molecule n during time step m, $\Delta\mathbf{r}_{mn}$, was random, uncorrelated with any of the other displacements $\Delta\mathbf{r}_{pq}$, and uniformly distributed on the surface of a sphere of radius Δr centred on the respective molecule. If the attempted step took the molecule into a fibre, then the position of the molecule at the end of step m was taken as the point of intersection of the attempted trajectory and the boundary of the fibre. The actual displacement $\Delta\mathbf{r}_{mn}$ was then re-calculated accordingly. If molecule n collided with a fibre in time step m, then in the time step m+1 the attempted displacement $\Delta\mathbf{r}_{m+1,n}$ was calculated according to the normal rules described above. If the attempted step $\Delta\mathbf{r}_{m+1,n}$ again took the molecule inside the fibre, the molecule remained stationary during that time step; otherwise, it restarted the random walk in the aqueous domain. After M time steps, the position of the n-th molecule was given by

$$\mathbf{r}_{Mn} = \mathbf{r}_{0n} + \sum_{m=1}^{M} \Delta\mathbf{r}_{mn} \tag{2}$$

Calculation of the diffusion tensor. At the end of each simulation, the apparent elements of the laboratory-frame (non-diagonalised) diffusion tensor were computed as

$$D_{ij} = \frac{1}{2 N_T \Delta t} \cdot \frac{1}{N_P} \sum_{n=1}^{N_P} \left(r^i_{N_T,n} - r^i_{0n} \right) \left(r^j_{N_T,n} - r^j_{0n} \right) \tag{3}$$

where the superscripts *i* and *j* refer to the *x*, *y*, or *z* components of the respective position vectors: e.g., $r^1_{\mathrm{NT},1} = x_{\mathrm{NT},1}$, etc.

The eigenvalues and eigenvectors of the diffusion tensor were obtained by Jacobi diagonalisation (Press et al. 1992) of the laboratory-frame tensor given by Eq. (3). The eigenvalue whose eigenvector $\mathbf{v}_i$ lay the closest to the *z* axis (i.e., max[$|\mathbf{v}_i \cdot \mathbf{k}|$]) was taken as the principal eigenvalue, D_1. The two remaining eigenvalues were taken as the secondary eigenvalues D_2 and D_3. This method of assigning the principal eigenvalue was used in order to avoid eigenvalue sorting bias (Basser and Pajevic 2000); it meant that, for a finite ensemble size N_P, D_1 could potentially be smaller than D_2 or D_3.

Fractional anisotropy. The fractional anisotropy (FA) of the diagonalised diffusion tensors was computed in accordance with the previously used definition (Meder et al. 2006):

$$\mathrm{FA} = \sqrt{\frac{3}{2}} \cdot \sqrt{\frac{(D_1 - D_{av})^2 + (D_2 - D_{av})^2 + (D_3 - D_{av})^2}{D_1^2 + D_2^2 + D_3^2}} \tag{4}$$

where D_{av} is the average diffusion coefficient:

$$D_{av} = \left(D_1 + D_2 + D_3\right)/3 \tag{5}$$

This definition of FA is designed for a prolate, axially symmetric diffusion tensor: $D_1 \geq D_2 = D_3$. In the limiting case $D_1 >> D_2, D_3$, FA takes the value of 1; in the case of isotropic diffusion ($D_1 = D_2 = D_3$), FA = 0.

RESULTS

Isotropic test: Diffusion tensor in bulk water. As a test of the random-walk procedure, the diffusion tensor was calculated from random walks simulated in bulk water (in the absence of collagen fibres). The input diffusion coefficient was $D_0 = 2.3 \times 10^{-3}$ mm^2 s^{-1}. In the first set of isotropic test simulations, 20 simulations were performed for the ensemble size $N_P = 95000$. In this set, the simulated eigenvalues of the DT were $(2.30 \pm 0.01) \times 10^{-3}$, $(2.30 \pm 0.02) \times 10^{-3}$, and $(2.30 \pm 0.01) \times 10^{-3}$ mm^2 s^{-1}; the simulated fractional anisotropy was 0.007 ± 0.002. In the second set, 20 simulations were performed for the ensemble size $N_P = 10^6$. In this set, the simulated eigenvalues of the DT were $(2.300 \pm 0.004) \times 10^{-3}$, $(2.300 \pm 0.004) \times 10^{-3}$, and $(2.300 \pm 0.004) \times 10^{-3}$ mm^2 s^{-1}; the simulated fractional anisotropy was 0.0022 ± 0.0008.

Volume fraction of collagen as a function of the fibre threshold parameter. The relationship between the fibre threshold parameter T and the volume fraction of collagen, ϕ, is illustrated in Fig. 2. This plot was used to translate the value of T (a computational parameter with no absolute physical meaning) into the value of ϕ (which provides a measure of the amount of collagen in the model tissue). In every simulation, the value of T used was converted into the corresponding value of ϕ using the values of the points shown in Fig. 2. Hence, in the following we refer to the dependence of the simulated DT on the collagen volume fraction (ϕ) rather than the fibre threshold parameter. The solid line shown in Fig. 2 is an approximation of $\phi(T)$ for the thin fibres; it was not used for the conversion.

In the 17 sets of anisotropic simulations performed, the values of T used were equidistant and ranged from 0 to 1.6. Because the relationship between T and ϕ was nearly linear, the corresponding ϕ values were spaced nearly equidistantly. The ϕ values ranged from 0.406 to 0.002.

DT eigenvalues as a function of collagen volume fraction. The dependence of the eigenvalues of the simulated diffusion tensor (D_i) on the collagen volume fraction (ϕ) is shown in Fig. 3. The values shown are the averages from the sets of 10 simulations performed for each value of ϕ. The simulated principal eigenvalue was $(2.30 \pm 0.01) \times 10^{-3}$ mm^2 s^{-1} at $\phi = 0.002$ and monotonically decreased to $(2.0 \pm 0.1) \times 10^{-3}$ mm^2 s^{-1} at $\phi = 0.406$. The secondary eigenvalues exhibited a

more pronounced decrease with the increasing fibre volume: from $(2.296 \pm 0.008) \times 10^{-3}$ mm^2 s^{-1} at $\phi = 0.002$ to $(1.51 \pm 0.06) \times 10^{-3}$ mm^2 s^{-1} at $\phi = 0.406$.

The principal eigenvector of the DT tended to be aligned along the *z* axis. For the relatively thick fibres ($T \leq 0.8$, $\phi \geq 0.197$), the principal eigenvector of 89 of the 90 simulated tensors lay within 5^o of the *z* axis. This trend also persisted for the thinner fibres: overall, the principal eigenvector of 135 of the 170 simulated tensors lay within 5^o of the *z* axis. The three eigenvectors of a given tensor were always perpendicular to each other within the rounding error. The secondary eigenvectors tended to be approximately uniformly distributed in the *xy* plane, with a slight preference for the directions along the *x*, *y* axes and at $\pm 45^o$ to the *x*, *y* axes.

Fractional Anisotropy as a function of collagen volume fraction. The dependence of the fractional anisotropy (FA) of the simulated diffusion tensor, defined according to Eq. (4), vs the volume fraction of collagen (ϕ) is shown in Fig. 4. The empirical form of this dependence was linear. The solid straight line shown in Fig. 4 represents the least-squares fit, $FA = 0.0046 + 0.5066\ \phi$. At the smallest and largest collagen volume fractions used, the respective simulated FA values were 0.008 ± 0.002 ($\phi = 0.002$) and 0.209 ± 0.003 ($\phi = 0.406$).

DISCUSSION

Magnetic resonance (MR) measurements of translational diffusion in biological tissues and materials can provide a wealth of information about the microscopic morphology of the sample (Cooke et al. 2009; Cox et al. 2009; de Visser et al. 2008a; Filidoro et al. 2005; Greene et al. 2008; Kuchel et al. 2000; Meder et al. 2006; Moffat and Pope 2002; Momot et al. 2004; Mori et al. 1999; Nucifora et al. 2007; Pierpaoli et al. 1996; Schwenzer et al. 2009; Silvast et al. 2009; Torres et al. 1999). Diffusion of water molecules in tissues can typically be described as restricted: the aqueous domain is confined by cell walls, fibres, or similar constraints (which for simplicity will be referred to as "walls"). The diffusing water molecules are free to move around the aqueous domain but are excluded from the confining walls. In this respect, diffusion of water in tissues is formally similar to diffusion in liquid-filled porous media (Callaghan et al. 1999; Mitra et al. 1992; Sen 2004). In isotropic (non-aligned) tissues such restricted diffusion is characterised by an apparent diffusion coefficient D_{app}, which is a function of the diffusion time (Δ). As Δ increases from 0 to infinity, the value of D_{app} monotonically decreases from the bulk-water diffusion coefficient (D_0) to the asymptotic, Δ-independent value D_∞. The slope of $D_{app}(\Delta)$ in the short-Δ limit is determined by the surface-to-volume ratio of the confinements, while the ratio D_∞/D_0 is determined by the tortuosity and the topology of the restricted aqueous domain (Mitra et al. 1992).

Many tissues (e.g., nerves, muscles, or articular cartilage) exhibit a well-defined direction of global alignment. Diffusion of water in such tissues is anisotropic – i.e., the magnitude of the characteristic displacement of the diffusing molecules is direction-dependent. Anisotropic diffusion is usually characterised by a diffusion tensor (DT) (Basser et al. 1994). Such diffusion is also restricted, and therefore the apparent diffusion tensor can be a function of the diffusion time. The eigenvalues of the DT characterise the diffusivity along and across the preferred direction of alignment, while the eigenvectors of the DT characterise the direction of the alignment relative to the laboratory reference frame.

In DTI of cartilage, the diffusion time (Δ) is typically determined by hardware and signal-to-noise considerations; the typical range of Δ is between 5 and 30 ms. This corresponds to an RMS translational displacement between ~3 and 12 μm, which is significantly larger than the characteristic separation between collagen fibres (Jeffery et al. 1991). This means that DTI

measurements sample the asymptotic (long-Δ) diffusion tensor. The MC simulations presented here also sampled the long-Δ DT. As seen from Fig. 1b, the RMS displacement of the tracer molecules exceeded the fibre separation even after 1/20 of the full simulation; at the end of the simulation ($\Delta = 1.5 \times 10^{-4}$ s) the RMS displacement of the tracers was $\approx \sqrt{2 D_0 \Delta} \sim 10 L_0$, which corresponds to "long" Δ. In this regime, the DT can be considered independent of Δ. It also means that the simulated diffusion tensor depends only on ϕ but not on the absolute size of the collagen fibres. As long as the RMS displacement of the tracers during Δ significantly exceeds L_0, the asymptotic long-Δ diffusion tensor is affected by the tortuosity of the aqueous domain but not by the absolute length scale of the fibre lattice.

The use of Eq. (1) implies that water diffusion in the aqueous domain was assumed to be Gaussian. This assumption did not extend to the restricted diffusion: the obstructive effect of collagen fibres resulted in an average diffusion propagator that did not follow a simple analytic form. For this reason, the elements of the diffusion tensor were extracted from the final positions of the tracer particles using Eq. (3). This approach is consistent with the established methodology used for simulations of diffusion in porous media (Regan and Kuchel 2002, 2003; Valiullin and Skirda 2001). Equation (3) is model-independent in the sense that no assumptions were made about the functional form of the restricted-diffusion propagator; the Equation also accurately reflects the physical meaning of the apparent diffusion tensor obtained from DTI measurements.

Interaction between water and collagen. In the model used, the collisions of tracer molecules with the fibres can be described as completely inelastic with weak absorption. A molecule encountering a fibre remains at its surface until the random Brownian forces impart to it a velocity vector that is directed away from the fibre. The colliding molecule in this model does not experience a strong attractive interaction with the fibre that would be sufficient to keep it in the absorbed state beyond a few time steps. However, weak hydrogen bonding between the water molecule and the fibre is assumed to be sufficient to suppress translational diffusion of the molecule while it remains on the fibre. The absorbed molecule has a finite residence time on the fibre surface (of the order of several time steps) because in a given time step the random Brownian forces have a comparable probability of being directed towards or away from the fibre. Therefore, despite the lack of strong absorptive interaction, the tracer molecules spend a finite fraction of time in the absorbed state. As a result, the observed diffusion coefficient in the

direction of fibre alignment (the unobstructed direction) can be expected to decrease linearly with the ratio (surface of the fibres):(volume of the aqueous domain). This ratio is proportional to the collagen volume fraction at low values of ϕ; therefore, the principal eigenvalue of the DT (which corresponds to diffusion along the fibres) should decrease with ϕ approximately linearly. This can indeed be seen from Fig. 3a. This decrease can be attributed to the "non-sticky" weak absorption model implicit in the simulations.

Obstructive effect of collagen fibres. The obstructive effect of collagen fibres on water diffusion is manifested in the behaviour of the secondary eigenvalues of the diffusion tensor (D_2 and D_3), which characterise diffusivity in the directions perpendicular to the fibres. In the limit of zero noise, these two eigenvalues should be equal due to the square symmetry of the fibre network. For this reason, D_2 and D_3 were treated as being fundamentally the same quantity. In Fig. 3a, D_2 and D_3 were averaged together in order to construct the plot of the secondary DT eigenvalue vs ϕ. The simulated secondary eigenvalue ($D_{2,3}$) exhibited a more pronounced decrease with the increasing ϕ than the principal eigenvalue (D_1). This can be explained as follows. The principal eigenvalue, D_1, decreases with ϕ due to weak absorption discussed in the previous paragraph. This reduction is not direction-specific; therefore, the secondary eigenvalues experience an identical relative decrease due to the same factor. However, the secondary eigenvalues also experience a decrease due to the obstructive effect of the collagen fibres, which restrict translational diffusion of the molecules in the *xy* plane. The difference between the ratios D_1/D_0 and $D_{2,3}/D_0$ is therefore a measure of the obstructive effect of the collagen fibres. In order to separate the obstructive effect, the secondary eigenvalues were corrected for the weak absorption and normalised by D_0:

$$D^*_{2,3} = \frac{D_0 - (D_1 - D_{2,3})}{D_0} \tag{6}$$

Attenuation of $D^*_{2,3}$ with the increasing ϕ represents the pure obstructive effect of the fibres. The natural log of $D^*_{2,3}$ is plotted vs ϕ in Fig. 3b; the plot can be seen to be linear. This corresponds to the Edwards-Freed behaviour of the obstructed diffusion coefficient (Cukier 1984). Plots of $\ln(D^*_{2,3})$ vs $\phi^{1/2}$, $\phi^{3/4}$, ϕ^2 and ϕ^3 were also examined; all of these plots were non-linear. The observed behaviour of the simulated $D^*_{2,3}$ is discussed below in the context of the available experimental data and analytic restricted-diffusion models.

Fractional anisotropy. The fractional anisotropy (FA) of the diffusion tensor, which is plotted in Fig. 4, exhibited a linear empirical relationship with the volume fraction of collagen (ϕ). It can be seen from the least-squares fit in Fig. 4 that the limiting FA at $\phi = 0$ exceeds zero. This is due to the finite size of the Monte Carlo ensemble ($N_P = 81910$) and can be understood as follows. The standard deviations of MC-sampled properties are inversely proportional to the square root of the ensemble size (Press et al. 1992); therefore, $\Delta D_i \propto 1/\sqrt{N_P}$. The errors ΔD_i in any finite-N_P simulation are positive; as a result, the values of D_1, D_2 and D_3 will always be unequal even in the isotropic case (in the absence of fibres). The fractional anisotropy defined by Eq. (4) is non-negative; for a finite N_P it is always positive, however small, as a result of statistical fluctuations of the D_i's. The situation is similar in experimental DTI measurements: the measured diffusion tensor of isotropic saline surrounding the cartilage possesses a "baseline" fractional anisotropy, typically in the range 0.01-0.05 (de Visser et al. 2008a; Meder et al. 2006). This can be understood through the analogy of calculating the average magnitude of white noise: while the average noise is zero, its average magnitude is positive and of the order of the noise RMS. Thus, the value FA = 0.0046 obtained for at $\phi = 0$ at $N_P = 81910$ is a "noise" fractional anisotropy. It can be expected to decrease with the increasing ensemble size because the standard deviations of the eigenvalues, ΔD_i, also decrease. This was indeed the case in the test isotropic simulations carried out at $N_P = 95000$ (FA = 0.007) and at $N_P = 1000000$ (FA = 0.002).

The plot of FA vs ϕ shown in Fig. 4 can be used as a "calibration curve" to convert the experimentally measured fractional anisotropy of the diffusion tensor into collagen volume fraction under the assumption of a regular lattice of perfectly aligned collagen fibres.

Effects of "bound" water and proteoglycans. MR properties of water in AC are usually explained in terms of rapid dynamic equilibrium between "free" water (which has the molecular hydrodynamic properties similar to those of bulk water) and water hydrogen-bonded to cartilage biopolymers ("bound" water) (Migchelsen and Berendsen 1973; Mlynarik et al. 2004; Momot et al. 2010):

$$\mathrm{H_2O} + \mathrm{P} \underset{k_-}{\overset{k_+}{\rightleftharpoons}} \mathrm{H_2O \cdots P} \qquad (7)$$

where ··· denotes hydrogen bonding and P stands for a biopolymer (either collagen or PG). A given water molecule therefore spends the fraction of its time $p_F = k_-/(k_- + k_+[P])$ in the bulk-like free state, where it possesses an intrinsic diffusion tensor $||\mathbf{D}_F||$. It is this intrinsic "free" tensor that was sampled in the MC simulations in this work. The remaining fraction of time, $p_B = 1 - p_F$, is spent in the biopolymer-bound state, where the water molecule possesses a zero diffusivity. Under rapid exchange, the measured diffusion tensor is the weighted-average of the two states and therefore scales proportionally to p_F:

$$\|\mathbf{D}\| = p_F \|\mathbf{D}_F\| \tag{8}$$

Each eigenvalue of the DT scales linearly with the molar fraction of "free" water according to Eq. (8). Because the fractional anisotropy given by Eq. (4) is invariant to the absolute scale of the DT, the introduction of chemical exchange given by Eq. (7) leaves the FA unchanged. Therefore, unlike the eigenvalues of the diffusion tensor, the *anisotropy* of the DT is invariant to the extent of hydrogen bonding between water and biopolymers (and to p_B). This provides the justification for neglecting proteoglycans (PGs) in the Monte Carlo model presented. Proteoglycans comprise between 5% and 10% of AC by weight and strongly influence the absolute diffusivity of water through hydrogen bonding. However, this influence is not direction-specific, and it was assumed that all eigenvalues of the DT are affected to the same relative extent, leaving FA unchanged. This assumption is borne out by the recent MR evidence that PGs do not possess global alignment (Deng et al. 2007) and do not contribute to the ordering of the surrounding water (Keinan-Adamsky et al. 2005). It is also supported by experimental DTI measurements of enzymatically degraded cartilage, where trypsin-induced PG depletion resulted in "no discernible change in FA profile" despite a 10-15% increase in the average diffusivity (Meder et al. 2006). The independence of FA of p_B is also supported by the available analytic models of anisotropic restricted diffusion in tissues (Hazlewood and Nicholson 1995), where both D_1 and $D_{2,3}$ scale as $(1 - p_B)$, resulting in no change in the fractional anisotropy. For these reasons, it was assumed that the aligned collagen fibres alone capture the essential features of the anisotropy of the DT. Therefore, while Fig. 4 was constructed for $p_B = 0$, it applies equally to the situation that includes the two-pool chemical exchange given by Eq. (7), as long as the intrinsic diffusivity of water in the biopolymer-bound pool is zero.

The presence of rapid exchange between "bound" and "free" water also simplifies the treatment of spin relaxation effects. Under rapid exchange, spin relaxation of water protons can be

characterised by a single relaxation rate: $R_2 = p_F R_{2F} + p_B R_{2B}$, where R_{2F} and R_{2B} are the intrinsic ^{1}H transverse relaxation rates in the "free" and "bound" water pools, respectively (Momot et al. 2010). Under this condition, spin relaxation can be omitted from the Monte Carlo simulations because the relaxation attenuation factor $\exp(-R_2\Delta)$ simply re-scales the ensemble-average transverse magnetisation in a way that is independent of the magnitude of the diffusion gradients or the diffusional displacements of tracer molecules.

Comparison with experimental data and analytic models. In a DTI study of bovine AC (de Visser et al. 2008a), the typical measured fractional anisotropy of the DT ranged from 0.08 ± 0.02 near the AS to 0.11 ± 0.04 near the bone. In the same measurements, the "noise" FA measured in the surrounding saline was 0.07 ± 0.02. In the limit of low noise and low FA, the measured FA is the sum of the "noise" FA and the intrinsic FA of the tissue; therefore, the intrinsic FA of AC ranged between 0.01 (near AS) and 0.04 (near bone). The experimentally measured diffusion tensor was axially symmetric within the accuracy of the measurements. The principal eigenvalue of the measured DT corresponds to the simulated D_1, while the two secondary (lower) eigenvalues correspond to $D_{2,3}$. The measured D_1 typically ranged from $(1.7 \pm 0.1) \times 10^{-9}$ m^2 s^{-1} near AS to $(1.2 \pm 0.2) \times 10^{-9}$ m^2 s^{-1} near the bone. The measured $D_{2,3}$ typically ranged from $(1.5 \pm 0.1) \times 10^{-9}$ m^2 s^{-1} near AS to $(1.0 \pm 0.2) \times 10^{-9}$ m^2 s^{-1} near the bone. The significant variation of the intrinsic FA across the depth of the cartilage cannot be attributed to differences between collagen content in the superficial and the radial zones, as the typical $\phi \approx 0.2$ in both zones (Xia 2000). It is also seen that the observed intrinsic FA in the radial zone (0.04) is significantly lower than the result of the perfect-alignment model (FA = 0.1 for $\phi = 0.2$). This can be attributed to the disorder in fibre alignment present in real AC. The presence of fibres of different orientations within a given volume element results in attenuation of the anisotropy of the DT. The presence of fibre alignment disorder is supported by the comparative study of AC using DTI and polarised light microscopy (PLM). The predominant direction of collagen fibre alignment determined from the two techniques was found to be correlated but not identical; this was attributed to the differences in the voxel sizes between PLM and DTI, resulting in different averaging behaviour of the alignment angle (de Visser et al. 2008a). Difference between the degree of collagen fibre alignment in different zones also appears to be the main factor responsible for the different FA values in the superficial and radial zones of AC. In the radial zone, where the alignment is relatively uniform, the observed FA is the greatest, while the

superficial and the transitional zones (where the collagen fibres are less ordered or completely disordered) exhibit the lowest FA.

In real AC, the variation of water diffusivity with the increasing biopolymer content can be attributed to two factors: (1) the increase in the fraction of "bound" water, and (2) the increasing obstructive effect of the biopolymer. In the simulations presented here, the attenuation of the simulated $D_{2,3}$ with the increasing ϕ was due almost entirely to the obstructive effect. This effect followed the Edward-Freed model, $D = D_0\, e^{-A\phi}$, as discussed under "Obstructive effect of collagen fibres". It is interesting to compare the simulated effect with the dependence of diffusivity on polymer content measured in related systems. Diffusion of water has been measured in a range of polymer hydrogels containing 5 – 60% (w/w) water (McConville and Pope 2000). Hydrogels are suitable systems for the comparison because the molecular hydrodynamics of water in AC is similar to that in hydrogels: as a result of rapid exchange of water molecules between bound and free environments, the diffusion coefficient of water is the weighted-average of the two populations. The observed D of water in hydrogels exhibited a behaviour of the type

$$D = D_0\, e^{-A\phi^3} \tag{9}$$

where ϕ was the polymer content. Diffusion of a range of probe molecules in poly(acrylamide) gels has also been measured; the diffusion coefficients of probe molecules exhibited a behaviour consistent with the de Gennes model (Tokita et al. 1996):

$$D = D_0\, e^{-AM^{1/4}\phi^{3/4}} \tag{10}$$

where M was the molecular weight of the probe molecule. The anisotropic case has been studied by Greene *et al* (Greene et al. 2010; Greene et al. 2008), who measured the diffusivities of water and 70 kDa dextran in compressed articular cartilage in the range of relative strains 0 – 0.7. This represents an indirect measurement of the dependence of the diffusivities on the biopolymer volume fraction (ϕ) because the strain of AC samples is linearly proportional to the water content. The diffusion coefficient of water was measured in the direction perpendicular to the articular surface and therefore corresponded to D_1 in this work. In different measurements, this diffusion coefficient decreased with the strain either linearly or as a non-linear function with a

negative curvature. The diffusion coefficient of dextran was measured parallel to the articular surface and therefore corresponded to $D_{2,3}$ in this work. It remained unchanged up to a certain threshold strain value, after which it decreased with the increasing strain approximately linearly. It can be seen from this collection of results that there does not appear to be a "universally applicable" behaviour of diffusion coefficients on the polymer volume fraction: the dependence $D(\phi)$ in different gel-like systems exhibited substantially different behaviours. This suggests that the obstructive effect of the polymer network is affected not only by the polymer content, but also by the morphology of the polymer network, including the spatial disorder of polymer molecules.

This hypothesis is supported by the results of Jóhannesson and Halle (Johannesson and Halle 1996), who compared numerical and analytic obstruction factors in ordered and disordered lattices of cylindrical fibres. In a regular square lattice, the transverse diffusion coefficient (equivalent to $D_{2,3}$) was shown to behave as

$$\frac{D}{D_0} = \frac{1}{1-\phi}\left(1-\frac{2\phi}{1+\phi-0.3\phi^4}\right) \tag{11}$$

in the range of ϕ from 0 to 0.4. Disordered square lattice exhibited lower obstruction factors (greater diffusion coefficients) for the equivalent values of ϕ. The importance of network morphology is also evident from the fact that a wide range of analytic models of restricted diffusion is available, and the validity of individual models depends on the macromolecular environment. Ogston et al (Ogston et al. 1973) used the Debye model,

$$D = D_0\, e^{-A\phi^{1/2}} \tag{12}$$

to describe transport of large particles through a solution of chain polymers. Cukier (Cukier 1984) used Debye model as well as Edward-Freed model, $D = D_0\, e^{-A\phi}$, and the de Gennes model given by Eq. (10). The applicability of these models was determined by the solvation state of the diffusing particles. Mackie-Meares model has also been used for polymers (Waggoner et al. 1993) and for articular cartilage (Knauss et al. 1999). However, the latter model appears to underestimate the water diffusion coefficient in AC. The values of $D_{2,3}$ obtained from DTI measurements of AC near the articular surface and in the radial zone were 0.65 D_0 and 0.43 D_0, respectively (de Visser et al. 2008a; Meder et al. 2006). The water volume fractions found in

these respective zones are 0.75 and 0.65 (Xia 2000), corresponding to the Mackie-Meares obstruction factor of 64% and 77% – i.e., the diffusion coefficients of 0.36 D_0 and 0.23 D_0. This model, therefore, underestimates the diffusion coefficient almost by a factor of 2. This underestimation is all the more significant because the model takes into account only the obstructive effect but not the "bound" water, p_B; when this is taken into account, the discrepancy between the Mackie-Meares model and the experimental measurements increases even further. The hard-sphere obstruction model, $D = D_0 (1 - 2\phi)$, which has been used for colloids and peptide solutions (Lekkerkerker and Dhont 1984; Momot and Kuchel 2006), similarly fails.

The simulated $D^*_{2,3}$ obtained in this work is consistent with the Edward-Freed model. Interestingly, none of the models discussed are consistent with the experimental results of McConville and Pope (McConville and Pope 2000) concerning diffusion of water in hydrogels. From a comparison of the empirical and theoretical models discussed above, it is apparent that capturing the characteristics of the disorder of the collagen network may be a requirement for accurate quantitative simulation of the anisotropy of the diffusion tensor in AC. The perfect-alignment, regular-lattice model used in the present work, therefore, provides only the first approximation in quantitative interpretation of DTI results of cartilage. Introduction of fibre alignment disorder and fibre grid disorder will be the subject of future work.

CONCLUSIONS

In this work, we used Monte Carlo simulations of Brownian dynamics of water to study anisotropic water diffusion in an idealised model of the radial zone of articular cartilage. The model consisted of a regular network of straight, mutually parallel collagen fibres arranged in a regular square grid. Chemical exchange between biopolymer-bound and free water was not considered because it has been shown not to affect the fractional anisotropy of the diffusion tensor. Under the assumptions used, the fractional anisotropy of the simulated diffusion tensor was linearly proportional to the collagen volume fraction. The work presented is the first step towards biophysical interpretation of MRI-measured diffusion tensor of water in articular cartilage. We hypothesise that extension of the present model to include fibre alignment disorder and fibre grid disorder can enable a quantitative interpretation of the experimentally measured diffusion tensor in articular cartilage.

Acknowledgements. This research was supported under Australian Research Council's Discovery Projects funding scheme (project number DP0880346). Supercomputer resources and services used in this work were provided by the High-Performance Computing Centre and Research Support Group (HPC), Queensland University of Technology. The supercomputing assistance provided by Mr Mark Dwyer (HPC) is gratefully acknowledged. The author thanks Mr Benjamin Harris, Ms Lucy Sim and Mr Samuel Trail for running preliminary Monte Carlo simulations of translational diffusion in model articular cartilage. The author thanks Profs James M. Pope and Sean McElwain and Dr Mark Wellard for useful discussions.

References

Avram L, Ozarslan E, Assaf Y, Bar-Shir A, Cohen Y, Basser PJ (2008) Three-dimensional water diffusion in impermeable cylindrical tubes: theory versus experiments. NMR Biomed. 21:888-898

Azuma T, Nakai R, Takizawa O, Tsutsumi S (2009) In vivo structural analysis of articular cartilage using diffusion tensor magnetic resonance imaging. Magn. Reson. Imaging 27:1242-1248

Basser PJ, Mattiello J, LeBihan D (1994) Estimation of the effective self-diffusion tensor from the NMR spin-echo. J. Magn. Reson. B 103:247-254

Basser PJ, Pajevic S (2000) Statistical artifacts in diffusion tensor MRI (DT-MRI) caused by background noise. Magn. Reson. Med. 44:41-50

Callaghan PT, Codd SL, Seymour JD (1999) Spatial coherence phenomena arising from translational spin motion in gradient spin echo experiments. Concepts Magn. Reson. 11:181-202

Cooke JM, Kalmykov YP, Coffey WT, Kerskens CM (2009) Langevin equation approach to diffusion magnetic resonance imaging. Phys. Rev. E 80:061102

Cox FM, Momot KI, Kuchel PW (2009) Magnetic-Resonance Evaluation of the Suitability of Microstructured Polymer Optical Fibers As Sensors for Ionic Aqueous Solutions. ACS Appl. Mater. Interfaces 1:197-203

Cukier RI (1984) Diffusion of Brownian spheres in semidilute polymer solutions. Macromolecules 17:252-5

de Visser SK, Bowden JC, Wentrup-Byrne E, Rintoul L, Bostrom T, Pope JM, Momot KI (2008a) Anisotropy of collagen fibre alignment in bovine cartilage: Comparison of polarised light microscopy and spatially-resolved diffusion-tensor measurements. Osteoarthr. Cartilage 16:689-697

de Visser SK, Crawford RW, Pope JM (2008b) Structural adaptations in compressed articular cartilage measured by diffusion tensor imaging. Osteoarthr. Cartilage 16:83-89

Deng X, Farley M, Nieminen MT, Gray M, Burstein D (2007) Diffusion tensor imaging of native and degenerated human articular cartilage. Magn. Reson. Imaging 25:168-171

Eyre DR, Wu JJ (2005) Collagen cross-links. Collagen, vol 247. Springer-Verlag Berlin, Berlin, pp 207-229

Filidoro L, Dietrich O, Weber J, Rauch E, Oerther T, Wick M, Reiser MF, Glaser C (2005) High-resolution diffusion tensor imaging of human patellar cartilage: Feasibility and preliminary findings. Magn. Reson. Med. 53:993-998

Freeman MAR (1979) Adult Articular Cartilage. Pitman Medical Publishing, England

Greene GW, Zappone B, Soderman O, Topgaard D, Rata G, Zeng HB, Israelachvili JN (2010) Anisotropic dynamic changes in the pore network structure, fluid diffusion and fluid flow in articular cartilage under compression. Biomaterials 31:3117-3128

Greene GW, Zappone B, Zhao B, Soderman O, Topgaard D, Rata G, Israelachvili JN (2008) Changes in pore morphology and fluid transport in compressed articular cartilage and the implications for joint lubrication. Biomaterials 29:4455-4462

Hazlewood CF, Nicholson C (1995) Diffusion in biological tissues. In: Le Bihan D (ed) Diffusion and Perfusion Magnetic Resonance Imaging. Raven Press, New York, pp 123-131

Jeffery AK, Blunn GW, Archer CW, Bentley G (1991) Three-dimensional collagen architecture in bovine articular cartilage. J. Bone Joint Surg.-Br. Vol. 73B:795-801

Johannesson H, Halle B (1996) Solvent diffusion in ordered macrofluids: A stochastic simulation study of the obstruction effect. J. Chem. Phys. 104:6807-6817

Keinan-Adamsky K, Shinar H, Navon G (2005) The effect of detachment of the articular cartilage from its calcified zone on the cartilage microstructure, assessed by H-2-spectroscopic double quantum filtered MRI. J. Orthop. Res. 23:109-117

Knauss R, Schiller J, Fleischer G, Karger J, Arnold K (1999) Self-diffusion of water in cartilage and cartilage components as studied by pulsed field gradient NMR. Magn. Reson. Med. 41:285-292

Kuchel PW, Durrant CJ, Chapman BE, Jarrett PS, Regan DG (2000) Evidence of red cell alignment in the magnetic field of an NMR spectrometer based on the diffusion tensor of water. J. Magn. Reson. 145:291-301

Landman BA, Farrell JAD, Smith SA, Reich DS, Calabresi PA, Zijl PCMv (2010) Complex geometric models of diffusion and relaxation in healthy and damaged white matter. NMR Biomed.:in press, DOI: 10.1002/nbm.1437

Lekkerkerker HNW, Dhont JKG (1984) On the calculation of the self-diffusion coefficient of interacting Brownian particles. J. Chem. Phys. 80:5790-5792

McConville P, Pope JM (2000) A comparison of water binding and mobility in contact lens hydrogels from NMR measurements of the water self-diffusion coefficient. Polymer 41:9081-9088

Meder R, de Visser SK, Bowden JC, Bostrom T, Pope JM (2006) Diffusion tensor imaging of articular cartilage as a measure of tissue microstructure. Osteoarthr. Cartilage 14:875-881

Migchelsen C, Berendsen HJC (1973) Proton exchange and molecular orientation of water in hydrated collagen fibers. NMR study of water and water-D2. J. Chem. Phys. 59:296-305

Mitra PP, Sen PN, Schwartz LM, Ledoussal P (1992) Diffusion propagator as a probe of the structure of porous-media. Phys. Rev. Lett. 68:3555-3558

Mlynarik V, Szomolanyi P, Toffanin R, Vittur F, Trattnig S (2004) Transverse relaxation mechanisms in articular cartilage. J. Magn. Reson. 169:300-307

Moffat BA, Pope JM (2002) Anisotropic water transport in the human eye lens studied by diffusion tensor NMR micro-imaging. Exp. Eye Res. 74:677-687

Momot KI, Kuchel PW (2006) PFG NMR diffusion experiments for complex systems. Concepts Magn. Reson. 28A:249-269

Momot KI, Kuchel PW, Whittaker D (2004) Enhancement of Na^+ diffusion in a bicontinuous cubic phase by the ionophore monensin. Langmuir 20:2660 - 2666

Momot KI, Pope JM, Wellard RM (2010) Anisotropy of spin relaxation of water protons in cartilage and tendon. NMR Biomed. 23:313–324

Mori S, Crain BJ, Chacko VP, van Zijl PCM (1999) Three-dimensional tracking of axonal projections in the brain by magnetic resonance imaging. Ann. Neurol. 45:265-269

Nieminen MT, Toyras J, Laasanen MS, Silvennoinen J, Helminen HJ, Jurvelin JS (2004) Prediction of biomechanical properties of articular cartilage with quantitative magnetic resonance imaging. J. Biomech. 37:321-328

Nucifora PGP, Verma R, Lee SK, Melhem ER (2007) Diffusion-tensor MR Imaging and tractography: Exploring brain microstructure and connectivity. Radiology 245:367-384

Ogston AG, Preston BN, Wells JD, Snowden JM (1973) Transport of compact particles through solutions of chain-polymers. Proceedings of the Royal Society of London, Series A: Mathematical, Physical and Engineering Sciences 333:297-316

Pierce DM, Trobin W, Raya JG, Trattnig S, Bischof H, Glaser C, Holzapfel GA (2010) DT-MRI based computation of collagen fiber deformation in human articular cartilage: a feasibility study. Ann. Biomed. Eng. 38:2447-2463

Pierce DM, Trobin W, Trattnig S, Bischof H, Holzapfel GA (2009) A Phenomenological Approach Toward Patient-Specific Computational Modeling of Articular Cartilage Including Collagen Fiber Tracking. J. Biomech. Eng. 131:091006

Pierpaoli C, Jezzard P, Basser PJ, Barnett A, DiChiro G (1996) Diffusion tensor MR imaging of the human brain. Radiology 201:637-648

Press WH, Teukolsky SA, Vetterling WT, Flannery BP (1992) Numerical Recipes in Fortran. Cambridge University Press, New York

Regan DG, Kuchel PW (2002) Simulations of molecular diffusion in lattices of cells: Insights for NMR of red blood cells. Biophys. J. 83:161-171

Regan DG, Kuchel PW (2003) Simulations of NMR-detected diffusion in suspensions of red cells: the "signatures" in q-space plots of various lattice arrangements. Eur. Biophys. J. Biophys. Lett. 31:563-574

Schwenzer NF, Steidle G, Martirosian P, Schraml C, Springer F, Claussen CD, Schick F (2009) Diffusion tensor imaging of the human calf muscle: distinct changes in fractional anisotropy and mean diffusion due to passive muscle shortening and stretching. NMR Biomed. 22:1047-1053

Sen PN (2004) Time-dependent diffusion coefficient as a probe of geometry. Concepts Magn. Reson. Part A 23A:1-21

Silvast TS, Kokkonen HT, Jurvelin JS, Quinn TM, Nieminen MT, Toyras J (2009) Diffusion and near-equilibrium distribution of MRI and CT contrast agents in articular cartilage. Phys. Med. Biol. 54:6823-6836

Tokita M, Miyoshi T, Takegoshi K, Hikichi K (1996) Probe diffusion in gels. Phys. Rev. E 53:1823-1827

Torres AM, Taurins AT, Regan DG, Chapman BE, Kuchel PW (1999) Assignment of coherence features in NMR q-space plots to particular diffusion modes in erythrocyte suspensions. J. Magn. Reson. 138:135-143

Valiullin R, Skirda V (2001) Time dependent self-diffusion coefficient of molecules in porous media. J. Chem. Phys. 114:452-458

Waggoner RA, Blum FD, Macelroy JMD (1993) Dependence Of The Solvent Diffusion-Coefficient On Concentration In Polymer-Solutions. Macromolecules 26:6841-6848

Xia Y (2000) Magic-angle effect in magnetic resonance imaging of articular cartilage - A review. Invest. Radiol. 35:602-621

Figure Captions

Fig. 1 An example of the collagen fibre lattice showing typical distributions of tracer particles: (a) at the start of a random walk; (b) the same tracers after the first 1500 steps of the random-walk simulation. The *x* and *y* axes of the coordinate system used in the simulations are shown in the drawing; the *z* axis was perpendicular to the plane of the drawing. The fibre cross-sections, implicitly defined by Eq. (13), can be seen to be nearly circular: the fibre radii measured along the *x* axis and at 45^{o} to the *x* axis differ by less than 4%. In the example shown, a small ensemble size ($N_P = 1000$) was used, the same time step $\Delta t = 5 \times 10^{-9}$ s as in the actual simulations, and the fibre threshold parameter $T = 0.8$. The actual simulations used $N_P = 81910$ tracers and $N_T = 30000$ time steps. The *z* positions were discarded in making these plots (i.e., the distributions shown are projections onto the *xy* plane).

Fig. 2 The relationship between the threshold parameter *T* and the volume fraction of collagen, ϕ. For each value of *T*, the corresponding value of ϕ was obtained numerically as described in Methods. The solid line is a plot of the function $\phi = 16 \cdot (193/120 - T)/21\pi$, which approximates $\phi(T)$ in the limit of thin fibres. This line was obtained analytically and is shown as a visual guide only. The conversion of *T* to ϕ was performed using the actual *T* and ϕ values corresponding to the points of the plot.

Fig. 3 (a) Eigenvalues of the simulated diffusion tensor as a function of the collagen volume fraction (ϕ): open circles, the principal eigenvalue (D_1); solid squares, the secondary eigenvalues (D_2, D_3). The eigenvalues plotted correspond to long diffusion times: $2\,D_0\,t_s >> L_0^2$. The typical 95% confidence interval approximately corresponds to the symbol size. The solid line corresponds to the input diffusion coefficient, $D_0 = 2.3 \times 10^{-3}$ mm^2 s^{-1}, and is given as a visual guide. The reduction in D_2, D_3 with the increasing ϕ is due mostly to the obstructive effect of the fibres. The reduction in D_1 is due to weak absorption of the tracer molecules on the fibre surface, as discussed in text. (b) $\ln(D^*_{2,3})$, as defined in Eq. (6), plotted vs ϕ. $D^*_{2,3}$ is the normalised secondary eigenvalue of the DT corrected for the weak absorption of water molecules. Its attenuation with the increasing ϕ therefore represents the pure obstructive effect of the fibres. The linear dependence of $\ln(D^*_{2,3})$ on ϕ corresponds to the Edwards-Freed behaviour (Cukier 1984).

Fig. 4 The fractional anisotropy of the simulated diffusion tensor as a function of the collagen volume fraction ϕ. The points simulated are shown as solid dots; the size of the symbols approximately corresponds to the typical 95% confidence interval. The solid line is the least-squares fit, FA = 0.0046 + 0.5066 ϕ. The non-zero FA in the limit $\phi = 0$ is due to the finite ensemble size N_P (see Discussion).

Appendix: Collagen fibre lattice used in the MC simulations

The surface of the fibres was defined as

$$\begin{aligned}&\cos\left(\frac{2\pi x}{L_0}\right)-\frac{81}{320}\cos^2\left(\frac{2\pi x}{L_0}\right)+\frac{1}{15}\cos^3\left(\frac{2\pi x}{L_0}\right)-\frac{3}{320}\cos^4\left(\frac{2\pi x}{L_0}\right)+\\&\cos\left(\frac{2\pi y}{L_0}\right)-\frac{81}{320}\cos^2\left(\frac{2\pi y}{L_0}\right)+\frac{1}{15}\cos^3\left(\frac{2\pi y}{L_0}\right)-\frac{3}{320}\cos^4\left(\frac{2\pi y}{L_0}\right)=T\end{aligned} \tag{13}$$

where the threshold parameter T determines the cross-sectional size of the fibres. Equation (13) represents a harmonic expansion of the boundary of a perfectly spherical fibre to the eighth-order term of the Taylor series. The resulting fibres have nearly circular cross-sections: the fibre radii measured along the x axis and at 45^o to the x axis differ by less than 4%. The valid range of T is from 0 (the thickest fibres possible) to 193/120 (infinitely thin fibres). The radius of the fibre measured in the x or y direction ($R_{x,y}$) is related to T as

$$\frac{R_{x,y}}{L_0}=\sqrt{\frac{16\pi^2}{21}\left(\frac{193}{120}-T\right)} \tag{14}$$

Equation (13) implicitly defines an infinite periodic lattice of fibres that extends over the entire xy plane. Therefore, this definition of the fibre network obviates the need for periodic boundary conditions. If, for a given point (x, y), the expression on the lhs of Eq. (13) exceeded T, the point (x, y) was considered to lie inside a fibre ("the fibre domain"); otherwise, the point (x, y) lay in the interstitial space ("the aqueous domain" or "pore space"). The volume fraction of collagen, ϕ, was computed numerically for 33 equidistantly spaced values of T ranging from 0 to 1.6 in steps of 0.05. For each value of T, the corresponding ϕ was obtained by sampling a uniform 1000 × 1000 grid of (x, y) points covering a single unit cell of the lattice. The calibration plot for conversion of T into ϕ and vice versa is shown in Fig. 2.

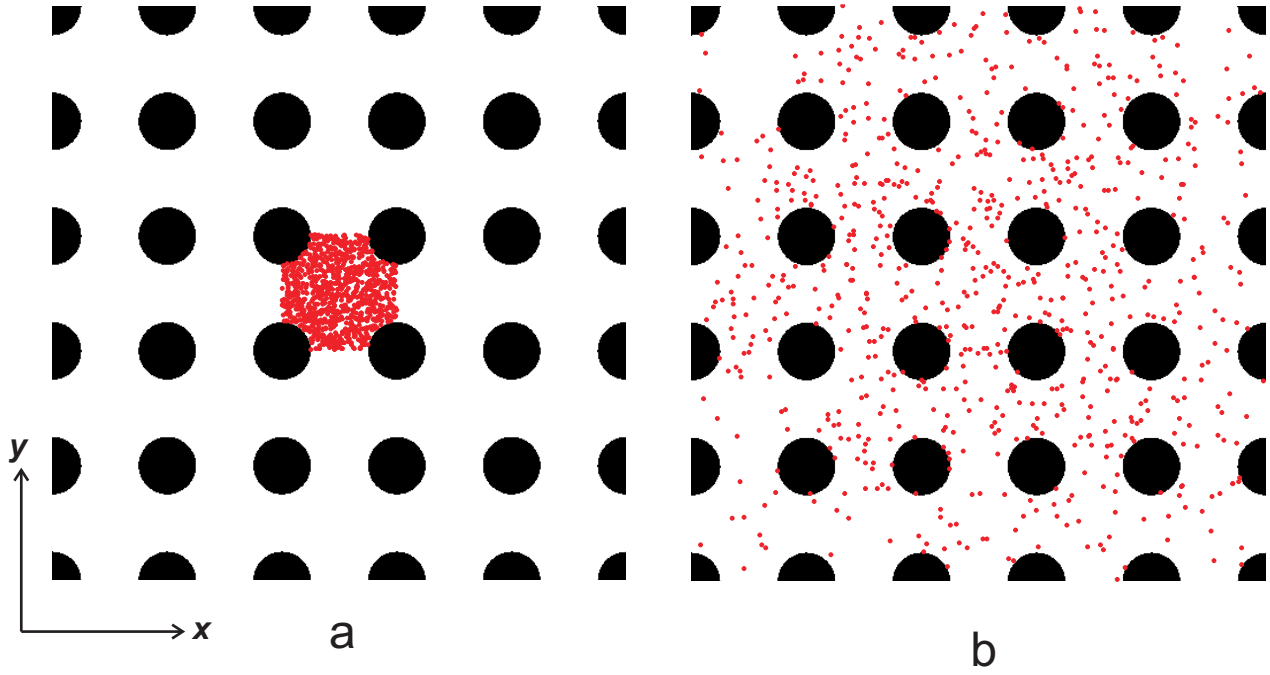

Figure 1, Momot KI

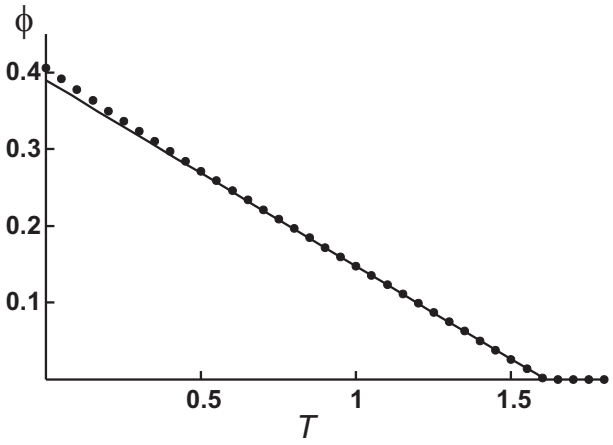

Figure 2, Momot KI

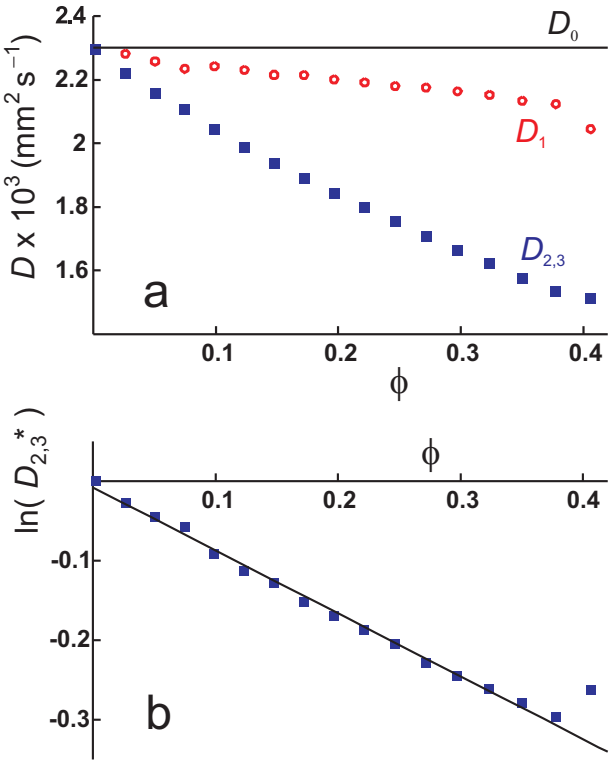

Figure 3, Momot KI

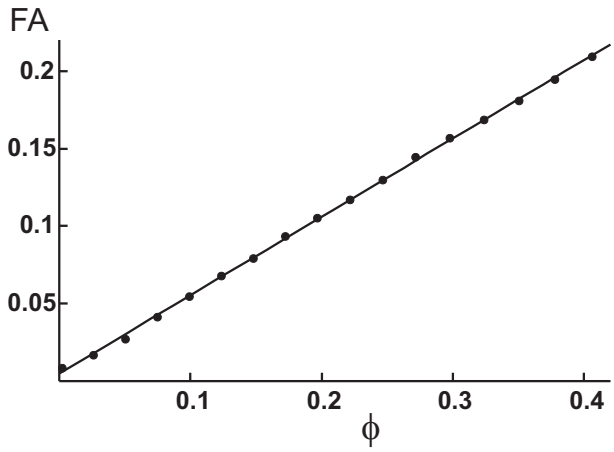

Figure 4, Momot KI